Synthesis and Reductive S–O Cleavage of Sulfur Oxide Clusters: $[PPN][HFe_3(CO)_9SO_2]$ and $[PPN]_2[Fe_3(CO)_9SO]$

G. B. Karet, C. L. Stern, D. M. Norton, and D. F. Shriver*

Contribution from the Department of Chemistry, Northwestern University. Evanston, Illinois 60208-3113

Received May 24, 1993®

Abstract: The cluster $[PPN][HFe_3(CO)_9SO_2]$ (**II**) was synthesized by reaction of $[PPN][HFe_3(CO)_{11}]$ (**I**) with SO_2 and was characterized by infrared spectroscopy, ^1H and ^{13}C NMR spectroscopy, X-ray crystallography, and cyclic voltammetry. The SO_2 ligand binds in an unusual μ_3-η^2 configuration and acts as a four-electron donor. The hydride ligand in **II** was detected by NMR spectroscopy, and a site for its location is evident in the structure. Acetylation of **II** followed by reduction with $NaPh_2CO$ yields the known sulfido cluster $[Fe_3(CO)_9S]^{2-}$ (**III**). Reduction of $[PPN][HFe_3(CO)_9SO_2]$ without prior acetylation leads to formation of $[PPN]_2[Fe_3(CO)_9SO]$ (**IX**). This cluster was characterized by infrared spectroscopy, NMR spectroscopy, and X-ray crystallography. $[PPN]_2[Fe_3(CO)_9SO]$ contains an SO ligand bonded symmetrically to all three iron atoms. Crystallographic data for **II**: space group $I2/a$, a = 36.565(9)Å, b = 13.756(2) Å, c = 17.648(4) Å, β = 90.87(2)°, V = 8876(6) Å^3. Crystallographic data for **IX**: space group Cc, a = 29.333(5) Å, b = 14.481(4) Å, c = 25.048(4) Å, β = 134.44(1)°.

Introduction

Mononuclear and dinuclear complexes with SO_2 ligands have been extensively studied.[1-3] Special interest has lain in the reduction of coordinated SO_2 to other sulfur oxides and S_8.[4,5] An interesting feature of SO_2 chemistry is that SO_2 exhibits a variety of bonding modes in mononuclear and dinuclear complexes. In mononuclear complexes the most common modes of coordination include η^1 planar coordination, as in $[CpMn(CO)_2(SO_2)]$,[7] η^1 pyramidal coordination, as in $[IrCl(CO)(PPh_3)_2(SO_2)]$,[8] and η^2 coordination, as in $[Rh(NO)(SO)_2(PPh_3)_2]$.[9] For two-metal systems and larger clusters, sulfur dioxide can bridge across a metal–metal bond, **IV**, or form an unsupported bridge between two metals, **V**. Normally, the SO_2 ligand bridges metals through only the S atom, as in $[Cp_2Fe(CO)_2]_2(SO_2)$.[10] Occasionally SO_2 may bridge through sulfur and oxygen, (**VI**), as in $[Mo(CO)_2(py)(SO_2)(PPh_3)]_2$.[11]

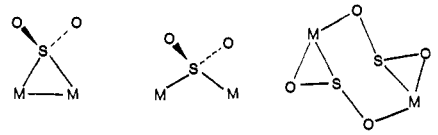

IV V VI

In comparison to mononuclear and dinuclear complexes, relatively few SO_2 cluster complexes containing three or more metal atoms are known. Most of those that have been structurally characterized are Pt or Pd clusters with phosphine ligands.[12-14] Few SO_2 complexes of metal carbonyl clusters have been crystallographically characterized, and of these, only three are anionic.[15-17] Only $[Au_2(PtCH_2PPh_2S)_4(SO_2)_2]$ contains an SO_2 ligand that does not bridge between metals.[14] Nucleophilic attack has been found to occur at S and electrophilic attack at O or S of coordinated SO_2 in mononuclear complexes.[18-21] However, to our knowledge, there are no examples of reduction of coordinated SO_2 in clusters of three or more metals. The exploration of the reactions of SO_2 on 3-metal systems is of interest from the standpoint of the role of multimetal interactions on the transformations of the SO_2 ligand.

We report here the synthesis and reactivity of a new cluster, $[PPN][HFe_3(CO)_9SO_2]$ (**II**), which has a sulfur dioxide bound in an unusual μ_3-η^2, geometry. Prompted by the well known

* Abstract published in *Advance ACS Abstracts*, October 1, 1993.

(1) Ryan, R. R.; Kubas, G. J.; Moody, D. C.; Eller, P. G. *Struct. Bonding (Berlin)*, **1981**, *46*, 47.
(2) Mingos, D. M. P. *Trans. Met. Chem. (Weinheim Ger.)* **1978**, *3*, 1.
(3) Schenk, W. A. *Angew. Chem. Int. Ed. Engl.* **1987**, *26*, 98.
(4) (a) Kubas, G. J.; Ryan, R. R. *J. Am. Chem. Soc.* **1985**, *107*, 6138. (b) Kubas, G. J.; Kubat-Martin, K. A. *J. Am. Chem. Soc.* **1989**, *111*, 7823.
(5) (a) Kubas, G. J.; Wasserman, J. H.; Ryan, R. R. *Organometallics* **1985**, *4*, 419. (b) Kubas, G. J.; Wasserman, H. J.; Ryan, R. R. *Organometallics* **1985**, *4*, 2012.
(6) Moody, D. C.; Ryan, R. R.; Salazar, K. V. *J. Catal.* **1981**, *70*, 221.
(7) Schilling, B. E. R.; Hoffman, R.; Lichtenberger, D. L. *J. Am. Chem. Soc.* **1979**, *101*, 585.
(8) (a) Vaska, L. *Acc. Chem. Res.* **1968**, *1*, 335. (b) LaPlaca, S. S.; Ibers, J. A. *Inorg. Chem.* **1966**, *5*, 405.
(9) Moody, D. C.; Ryan, R. R. *Inorg. Chem.* **1977**, *16*, 2473.
(10) (a) Reich-Rohwig, P.; Clark, A. C.; Downs, R. L.; Wojcicki, A. *J. Organomet. Chem.* **1978**, *145*, 57. (b) Churchill, M. R.; DeBoer, B. G.; Kalra, K. L. *Inorg. Chem.* **1973**, *12*, 1646. (c) Churchill, M. R.; DeBoer, B. G.; Kalra, K. L.; Reich-Rohwig, P.; Wojcicki, A. *J. Chem. Soc.* **1972**, 981.
(11) Jarvinen, G. J.; Kubas, G. J.; Ryan, R. R. *J. Chem. Soc., Chem. Commun.* **1981**, 305.
(12) (a) Briant, C. E.; Evans, D. G.; Mingos, D. M. P. *J. Chem. Soc., Chem. Commun.* **1982**, 1144. (b) Briant, C. E.; Evans, D. G.; Mingos, D. M. P. *J. Chem. Soc., Dalton Trans.* **1986**, 1535. (c) Hallam, M. F., Howells, N. D., Mingos, D. M. P., Wardle, R. W. M. *J. Chem. Soc., Dalton Trans.* **1985**, 845. (d) Mingos, D. M. P., Wardle, R. W. M. *J. Chem. Soc., Dalton Trans.* **1986**, *73*. (e) Mingos, D. M. P., Oster, P.; Sherman, D. J. *J. Organomet. Chem.* **1987**, *320*, 257. (f) Bott, S. G.; Hallam, M. F.; Ezomo, O. J.; Mingos, D. M. P.; Williams, I. D. *J. Chem. Soc., Dalton Trans.* **1988**, 1461. (g) Evans, D. G.; Hughes, G. R.; Mingos, D. M. P.; Bassett, J.-M.; Welch, A. J. *J. Chem. Soc., Chem. Commun.* **1980**, 1255. (h) Moody, D. C.; Ryan, R. R. *Inorg. Chem.*, **1977**, *16*, 1052. (i) Bott, S. G.; Burrows, A. D.; Ezomo, O. J.; Hallam, M. F.; Jeffry, J. G.; Mingos, D. M. P. *J. Chem. Soc., Dalton Trans.* **1990**, 3335.
(13) Bott, S. G.; Ezomo, O. J.; Mingos, D. M. P. *J. Chem. Soc., Chem. Commun.* **1988**, 1048.
(14) King, C.; Heinrich, D. D.; Garzon, G.; Wang, J.-C.; Fackler, J. P., Jr. *J. Am. Chem. Soc.* **1989**, *111*, 2300.
(15) Briant, C. E.; Theopold, B. R. C.; Mingos, D. M. P. *J. Chem. Soc., Chem. Commun.* **1981**, 963.
(16) (a) Braga, D.; Ros, R., Roulet, R. *J. Organomet. Chem.*, **1985**, *286*, C8. (b) Ewing, P.; Farrugia, L. J. *Organometallics* **1989**, *8*, 1665. (c) Jarvinen, G. D.; Ryan, R. R. *Organometallics* **1984**, *3*, 1434.
(17) Bogdan, P. L.; Sabat, M.; Sunshine, S. A.; Woodcock, C.; Shriver, D. F. *Inorg. Chem.* **1988**, *27*, 1904.
(18) (a) Schenk, W. A.; Urban, P.; Stährfeldt, T.; Dombrowski, E. *Z. Naturforsch.* **1992**, *47b*, 1493. (b) SchenkW. A.; Karl, U. *Z. Naturforsch.* **1989**, *44b*, 993. (c) Glen, K.; Breuel, W. *Z. Anorg. Allg. Chem.* **1938**, *235*, 211. (d) Braga, D.; Ros, R. Roulet, R. *J. Organomet. Chem.*, **1985**, *286*, C8.
(19) (a) Reich-Rohrwig, P.; Clark, A. C.; Downs, R. L.; Wojcicki, A. *J. Organomet. Chem*, **1978**, *145*, 57. (b) Jablonski, C. R. *J. Organomet. Chem.*, **1977**, *142*, C25. (c) Thomasson, J. E.; Robinson, P. W.; Ross, D. A.; Wojcicki, A. *Inorg. Chem.* **1971**, *10*, 2130. (d) Downs, R. L.; Wojcicki, A. *Inorg. Chim. Acta* **1978**, *27*, 91.
(20) Moody, D. C.; Ryan, R. R. *J. Chem. Soc. Chem. Commun.* **1980**, 1230.
(21) Schenk, W. A.; Baumann, F. E. *J. Organomet. Chem.* **1984**, *260*, C6.

0002-7863/93/1515-9979$04.00/0

acetylation and reductive cleavage of bridging CO ligands in $[PPN]_2[Fe_4(CO)_{13}]$ and $[PPN]_2[M_3(CO)_{11}]$ (M = Fe, Ru, Os), eqs 1 and 2, the acetylation and reduction of **II** was explored.[22]

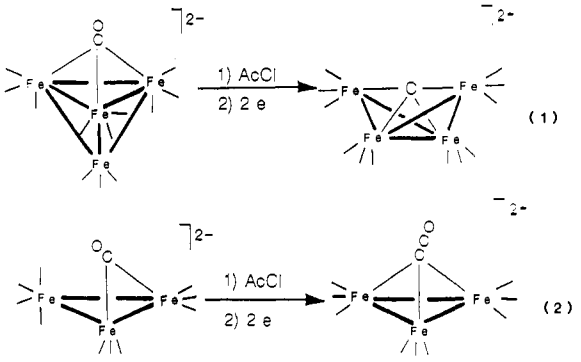

Even rarer than SO_2 complexes of clusters are polynuclear complexes of the reduced sulfur oxide ligand SO.[3] A major reason for the scarcity of SO complexes is the instability of free SO.[23] Although formation of free SO may occur by several routes, it readily decomposes to S or S_2O and SO_2.[23] Like O_2 and S_2, SO has been found to have a triplet ground state.[24] It has a S–O stretch at 1123.7 cm^{-1}, a S–O distance of 1.4809 + 0.001 Å, and a bond order of 1.98.[25] In the known mononuclear and dinuclear SO complexes, SO has been found to display several bonding modes. Mononuclear complexes such as $[Ir(SO)(PiCy_3)_2Cl]$ contain SO in a bent, η^1 geometry, where it serves as a 2-electron donor.[26] SO bridges two or more metals through sulfur in the dinuclear and polynuclear complexes $[MnCp(CO)_2]_2SO$ and $[Fe_3(CO)_9S(SO)]$.[3,27,28] In $[(P_3Rh)_2(SO)_2]$ (P_3 = 1,1,1-tris(diphenylphosphinomethyl)ethane), SO binds through both S and O.[29] The usual routes to SO complexes are the decomposition of coordinated thiirane *S*-oxide, C_2H_4SO,[3,26] reaction of metal complexes with $SOCl_2$,[30-32] or oxidation of sulfide ligands.[3,27-29]

A second goal of this research has been the synthesis of reduced sulfur oxide cluster complexes. It was anticipated that reductive S–O cleavage might serve as a systematic, high yield route to SO complexes. This expectation was borne out in the present work by the synthesis of the SO complex $[PPN]_2[Fe_3(CO)_9SO]$ (**IX**) by the reduction of coordinated SO_2 in $[PPN][HFe_3(CO)_9SO_2]$.

Experimental Section

General. All manipulations were carried out with the use of standard Schlenk techniques under an atmosphere of prepurified N_2 or on a high-vacuum line.[33] Solids were handled in the oxygen-free N_2 atmosphere of a drybox. Solvents were distilled from appropriate drying agents before use.[34] Solution infrared spectra were recorded on a Bomem MB-Series FTIR spectrometer at 2 cm^{-1} resolution with 0.1 mm path length CaF_2 solution cells. ^1H and ^{13}C NMR spectra of ^{13}C-labeled compounds were recorded on a Varian XL-400 spectrometer operating at 400 and 100 MHz, respectively. CD_2Cl_2 was vacuum distilled from P_4O_{10} before use, and it served as an internal NMR reference. FAB mass spectra, obtained by Cs^+ bombardment of samples in a *m*-nitrobenzyl alcohol matrix, were recorded by Dr. Hung of Northwestern University Analytical Services Laboratory. Elemental analysis was done by Elbach Analytical Laboratories, Engelskirchen, Germany. Space filling models were generated with SYBYL on a Silicon Graphics Indigo Workstation.

Noncondensible gases were removed from frozen SO_2 (Matheson) under vacuum before its use. $CH_3C(O)Cl$ was purified by vacuum distillation from PCl_5 and quinoline. Sodium beads were washed with pentane and stored in a glove box until use. Benzophenone and CO were used without purification. $[PPN][HFe_3(CO)_{11}]$ (**I**) was synthesized according to literature procedures.[35]

Synthesis of $[PPN][HFe_3(CO)_9SO_2]$ (II). A 30- mL Schlenk flask fitted with a vacuum line adapter and a stir bar was charged with 1.43 g (1.41 mmol) of $[PPN][HFe_3(CO)_{11}]$. THF (20 mL) was added. The solution was freeze–pump–thaw degassed and SO_2 (2.70 equiv) was condensed on the frozen pink solution. The solution was thawed and allowed to stir overnight, during which time it bubbled and turned orange red. Diethyl ether (40 mL) was then added. The red solution was filtered from the resulting orange brown solids, which were washed with 2 × 20 mL of Et_2O to extract any remaining product. After addition of 20 mL of pentane the volume of the filtrate was reduced to ca. 50 mL. Dropwise addition of 80 mL of pentane gave red crystals. Yield 810 mg, 56%. IR(ν(CO), THF) 2061 (w), 2017 (vs), 1998 (vs), 1977 (s), 1959 (m) cm^{-1}. IR (ν(SO), Nujol mull) 1143, 929 cm^{-1}. ^1H NMR (20 °C, CD_2Cl_2) −15.74 ppm. ^{13}C NMR (20 °C, CD_2Cl_2) δ 216 (br), 213.9, 205 (br) ppm. ^{13}CNMR (−90 °C, CD_2Cl_2) δ 216.45(1), 215.55(2), 215.18(2), 211.14(2), 203.29(2) ppm. FAB-MS P = 485 (R_p< 0.01) with loss of 9 CO ligands and SO_2. Anal. Calcd: C, 52.7; H, 3.03; N, 1.37; S, 3.14; Fe, 17.3. Found: C, 52.54; H, 3.22; N, 1.39; S, 3.18; Fe, 16.75.

Attempted Reaction of $[PPN]_2[HFe_3(CO)_9SO_2]$ (II) with CO. A 30-mL Schlenk flask was charged with 50 mg of $[PPN]_2[HFe_3(CO)_9SO_2]$ and a stir bar. After addition of 10 mL of THF, the solution was freeze–pump–thaw degassed. Carbon monoxide (5 psig) was added. The infrared spectrum indicated no reaction had occurred after the solution was allowed to stir for 32 h.

Acetylation and reduction of $[PPN][HFe_3(CO)_9SO_2]$. A 100-mL Schlenk flask was charged with 200 mg of $[PPN][HFe_3(CO)_9SO_2]$ and 20 mL of THF was added, followed by 200 μL of AcCl. The red solution turned orange brown after being stirred for 1 h. An infrared spectrum of the reaction mixture taken at this point revealed ν(CO) 2080 (w), 2062 (m), 2047 (s), 2006 (s), 1979 (m) 1962 (w), 1908, 1748 cm^{-1}. A reducing solution, made from 0.4 g of Na and 1.5 g of benzophenone in 20 mL of THF, was added until solids precipitated, giving a muddy brown suspension. The solvent was removed in vacuo. From the resulting oily solids an orange brown solution was extracted with 20 mL of CH_2Cl_2. Slow diffusion of 40 mL of Et_2O into the CH_2Cl_2 solution produced red needles of $[Na]_x[PPN]_{2-x}[Fe_3(CO)_9S]$ (**III**) cocrystallized with NaOAc. Yield 85 mg. IR (ν(CO), CH_2Cl_2) 1998 (w), 1928 (vs), 1899 (s), 1872-(m) cm^{-1}. ^{13}C NMR (CD_2Cl_2, −90 °C) 221.16 ppm from TMS.

Small-Scale Reaction of $[PPN][HFe_3(CO)_9SO_2]$ with AcCl. In a typical reaction, 50 mg of $[PPN][HFe_3(CO)_9SO_2]$ in a 5-mm NMR tube covered with a rubber septum was dissolved in CD_2Cl_2. Acetyl chloride (40 μL) was added and the tube was shaken. As soon as the color changed from red to orange brown, the tube was placed in the probe of an NMR spectrometer and ^1H and ^{13}C spectra were acquired. The presence of paramagnetic decomposition products, indicated by a shift of the solvent ^1H resonance of ca. 3 ppm, sometimes broadened resonances attributed to the cluster. Two products were observed. **VII**:^1H (CD_2Cl_2, 25 °C) 2.23, −24.44 ppm; ^{13}C (25 °C) 202.54, 167.29, 20.49 ppm. **VIII**:^1H (CD_2Cl_2, 25 °C) 2.25, −22.75 ppm; ^{13}C (−40 °C) 210.40, 166.78, 20.2, ppm; ^{13}C (−90 °C, CD_2Cl_2) 215 (br, 2), 209 (br, 7) ppm.

Synthesis of $[PPN]_2[Fe_3(CO)_9SO]$ (IX). A 100-mL Schlenk flask was charged with 280 mg (0.273 mmol) of $[PPN][HFe_3(CO)_9SO_2]$ and a stir

(22) (a) Kolis, J. W.; Holt, E. M.; Drezdzon, M. A.; Whitmire, K. H.; Shriver, D. F. *J. Am. Chem. Soc.* **1982**, *104*, 6134. (b) Sailor, M. J.; Brock, C. P.; Shriver, D. F. *J. Am. Chem. Soc.* **1987**, *104*, 6015. (c) Went, M. J.; Sailor, M. J.; Bogdan, P. L.; Brock, C. P.; Shriver, D. F. *J. Am. Chem. Soc.* **1987**, *109*, 6023. Ceriotti, A.; Chini, P.; Longoni, G.; Piro, G. *Gazz. Chim. Ital.* **1982**, *112*, 353.

(23) (a) *Gmelin Handbuch der Anorganischen Chemie*, 8th ed. (Schwefel, Ergänzungsband 3); Springer: Berlin, 1980. (b) Schenk, P. W.; Steudel, R. *Angew. Chem., Int. Ed. Engl.* **1965**, *4*, 402. (c) Schenk, P. W.; Steudel, R. In *Inorganic Sulfur Chemistry*; Nickless, G., Ed.; Elsevier: Amsterdam, 1968.

(24) (a) Daniels, J. M.; Dorain, P. B. *J. Chem. Phys.* **1966**, *45*, 26. (b) Carrington, A.; Levy, D. H. *J. Phys. Chem.* **1967**, *71*, 2.

(25) (a) Amano, T.; Hirota, E.; Morino, Y. *J. Phys. Soc. Jpn.* **1967**, *22*, 399. (b) Martin, E. V. *Phys. Rev.* **1932**, *41*, 167.

(26) Schenk, W. A.; Leissner, J.; Burschka, C. *Angew Chem., Int. Ed. Engl.* **1984**, *23*, 806.

(27) (a) Markó, L.; Markó-Monostory, B.; Modach, T.; Vahrenkamp, H. *Angew. Chem., Int. Ed. Engl.* **1980**, *19*, 226. (b) Lorenz, I.-P.; Messelhäuser, J. *Z. Naturforsch.* **1984**, *B39*, 403.

(28) (a) Lorenz, I.-P.; Messelhäuser, J.; Hiller, W.; Haug, K. *Angew. Chem., Int. Ed. Engl.* **1985**, *24*, 228. (b) Höfler, M.; Baitz, A. *Chem. Ber.* **1976**, *109*, 3147.

(29) Bianchini, C.; Mealli, C.; Meli, A.; Sabat, M. *J. Chem. Soc., Chem. Commun.* **1985**, 1024.

(30) Lorenz, I.-P.; Messelhäuser, J.; Hiller, W.; Conrad, M. *J. Organomet. Chem.* **1986**, *316*, 121.

(31) Lorenz, I.-P.; Hiller, W.; Conrad, M. *Z. Naturforsch.* **1985**, *40b*, 1383.

(32) Winter, A.; Zsolnai, L.; Hüttner, G. *J. Organomet. Chem.* **1982**, *234*, 337.

(33) Shriver, D. F.; Drezdzon, M. A. *The Manipulation of Air-Sensitive Compounds*, 2nd ed.; Wiley: New York, 1986.

(34) Gordon, A. J.; Ford, R. A. *The Chemist's Companion*; Wiley: New York, 1972.

(35) Hodali, H. A.; Arcus, C.; Shriver, D. F. *Inorg. Synth.* **1980**, *20*, 218.

Table I. X-ray Crystal Structure Data for [PPN]{$HFe_2(CO)_9SO_2$]

formula	$Fe_3SP_2O_{11}NC_{45}H_{31}$
M	1023.29
cryst size, mm	0.200 × 0.200 × 0.200
cryst system	monoclinic
space group	$I2/a$ (#15)
a, Å	36.565(9)
b, Å	13.756(2)
c, Å	17.648(4)
β, deg	90.87(2)
V, Å^3	8876(6)
Z	8
d(calc), g cm^{-3}	1.531
μ(Mo Kα), cm^{-1}	11.42
radiation	Mo Kα (λ = 0.71069 Å)
scan type	ω–θ
2θ max, deg	46.9
unique data	6867
obsd data, (I) > 3σ(I)	2179
no. of variables	344
reflcn/parameter ratio	6.33
$R(F)$	0.055
$R_w(F)$	0.049
GOF	1.35

bar. The cluster was dissolved in 20 mL of THF. A reducing solution of $NaPh_2CO$ in THF was added until IR spectra indicated completion of reaction. The solvent was removed in vacuo, and the product was extracted with 17 mL of acetone. Slow diffusion of 20 mL of Et_2O into the acetone solution produced maroon crystals. Yield 200 mg (47%). IR (ν(CO), THF) 2021 (w), 1955 (vs), 1943 (s), 1930 (m), 1897 (w), 1730 (vw, br) cm^{-1}. IR (Nujol mull ν(SO)), 1038 cm^{-1}. ^{13}C NMR (25 °C, CD_2Cl_2) 221.8(9), 219.7(5) ppm. Anal. Calcd: C, 62.9, H, 3.89; Fe, 10.8; S, 2.07. Found: C,61.36; H, 3.82; S, 2.91; Fe 10.75.

Electrochemical Measurements. Electrochemical measurements were performed using a BAS-100B electrochemical analyzer in a Schlenk-adapted two-compartment cell. Cyclic voltammograms were performed in acetonitrile solutions containing 0.27 M Bu_4NPF_6. Both Pt and glassy carbon disk working electrodes were employed with a Pt flag counter electrode and an Ag wire reference electrode. Electrode performance was monitored by observation of the ferrocene (Fc+/Fc) couple. Half wave potentials were taken as the average of the anodic and cathodic peak potentials for reversible couples. The same results were obtained with the carbon and platinum working electrodes.

Crystal Structure of [PPN][$HFe_3(CO)_9SO_2$]. A red, prismatic crystal of [PPN][$HFe_3(CO)_9SO_2$] was cut from a larger crystal grown by slow diffusion of pentane into a solution of **II** in a 1:2 Et_2O–THF mixture. This crystal was mounted on a glass fiber using oil (paratone-N, Exxon) and transferred to the cold stream (−120 °C) of an Enraf-Nonius CAD4 diffractometer with a Mo Kα radiation source. A summary of the data collection is given in Table I. The intensities were weak. Unit cell constants were determined by least-squares refinement of the setting angles of 25 unique reflections. Lorenz polarization and analytical absorption corrections were applied with transmission between 0.80 and 0.83 and an extinction correction was refined to 2.07 × 10^{-9}. A decay correction was not applied because the intensities of the three reflections monitored showed negligible variation.

Calculations were performed with the Texsan 5.0 crystallographic software package on a Micro Vax 3600 computer. The structure was solved by direct methods (Shelxs-86), with full-matrix least squares refinement. Carbon atoms in the cluster were refined isotopically; the remaining non-hydrogen atoms were refined with anisotropic thermal parameters. The maximum peak in the final difference map was 0.52 e/Å^3 and the minimum −0.50 e/Å^3. The final positional parameters of significant atoms are listed in Table II.

Crystal Structure of [PPN]$_2$[$Fe_3(CO)_9SO$] (IX). A red, equidimensional crystal grown by diffusion of pentane into an acetone solution of the cluster was mounted on a glass fiber using oil and transferred to the Enraf-Nonius CAD4 diffractometer. A summary of the data collection is given in Table V. Unit cell constants were determined as for **II**. Lorenz polarization and analytical absorption corrections were applied with transmission between 0.72 and 0.80, and an extinction correction was refined to 1.90 × 10^{-8}. A decay correction was not applied because the intensities of the three reflections showed negligible variation.

Calculations were performed as for **II**. The structure was solved by direct methods, with full-matrix least squares refinement. All non-hydrogen atoms were refined anisotropically. The minimum and maximum peaks in the final difference map are −0.40 and +0.38 e$^-$/Å^3, respectively. Positional parameters of significant atoms are shown in Table VI.

Table II. Positional Parameters of Significant Atoms for [PPN][$HFe_3(CO)_9SO_2$]

atom	X	Y	Z
Fe(1)	0.39730(5)	0.2530(2)	0.4163(1)
Fe(2)	0.39999(5)	0.2544(2)	0.2664(1)
Fe(3)	0.33731(5)	0.2396(2)	0.3340(1)
S	0.3957(1)	0.1317(3)	0.3401(2)
O	0.3535(3)	0.0953(7)	0.3339(6)
O(1)	0.4200(3)	0.0499(6)	0.3430(5)
O(11)	0.4712(3)	0.2269(8)	0.4791(5)
O(12)	0.3599(3)	0.1448(8)	0.5351(6)
O(13)	0.3830(3)	0.4488(7)	0.4762(5)
O(21)	0.3641(3)	0.1552(8)	0.1405(6)
O(22)	0.3944(3)	0.4546(7)	0.2102(5)
O(23)	0.4743(2)	0.2231(7)	0.2108(5)
O(31)	0.2832(3)	0.219(1)	0.4545(7)
O(32)	0.3318(3)	0.4481(8)	0.3551(6)
O(33)	0.2861(3)	0.238(1)	0.2032(6)
C(11)	0.4425(4)	0.237(1)	0.4549(8)
C(12)	0.3740(4)	0.190(1)	0.4880(9)
C(13)	0.3888(4)	0.373(1)	0.4524(8)
C(21)	0.3764(4)	0.196(1)	0.1909(8)
C(22)	0.3953(4)	0.375(1)	0.2330(8)
C(23)	0.4456(3)	0.236(1)	0.2341(7)
C(31)	0.3042(5)	0.222(1)	0.406(1)
C(32)	0.3352(4)	0.362(1)	0.3354(9)
C(33)	0.3059(4)	0.232(1)	0.2545(9)

Table III. Selected Bond Distances (Å) for [PPN][$HFe_3(CO)_9SO_2$]

Fe1–Fe2	2.649(3)	Fe2–C22	1.77(1)	O11–C11	1.14(1)
Fe1–Fe3	2.619(3)	Fe2–C23	1.79(1)	O12–C12	1.16(2)
Fe1–S	2.144(5)	Fe3–S	2.602(5)	O13–C13	1.14(1)
Fe1–C11	1.79(1)	Fe3–O	2.07(1)	O21–C21	1.13(1)
Fe1–C12	1.77(2)	Fe3–C31	1.78(2)	O22–C22	1.16(1)
Fe1–C13	1.80(1)	Fe3–C32	1.69(2)	O23–C23	1.15(1)
Fe2–Fe3	2.608(3)	Fe3–C33	1.80(2)	O31–C31	1.16(2)
Fe2–S	2.138(4)	S–O	1.62(1)	O32–C32	1.19(2)
Fe2–C21	1.77(1)	S–O1	1.434(9)	O33–C33	1.15(2)

Table IV. Selected Bond Angles (deg) for [PPN][$HFe_3(CO)_9SO_2$]

Fe2–Fe1–Fe3	59.34(7)	Fe1–S–Fe2	76.5(1)
Fe2–Fe1–S	51.7(1)	Fe1–S–Fe3	66.2(1)
Fe3–Fe1–S	65.3(1)	Fe1–S–O	107.3(4)
Fe1–Fe2–Fe3	59.74(7)	Fe1–S–O1	125.3(5)
Fe1–Fe2–S	51.9(1)	Fe2–S–Fe3	65.9(1)
Fe3–Fe2–S	65.6(1)	Fe2–S–O	106.3(4)
Fe1–Fe3–Fe2	60.91(7)	Fe2–S–O1	126.2(5)
Fe1–Fe3–S	48.5(1)	Fe3–S–O	52.7(4)
Fe1–Fe3–O	80.2(3)	Fe3–S–O1	163.0(5)
Fe2–Fe3–S	48.5(1)	O–S–O1	110.3(6)
Fe2–Fe3–O	79.7(3)	Fe3–O–S	88.7(5)
S–Fe3–O	38.6(3)		

Results and Discussion

Synthesis and Structure of [PPN][$HFe_3(CO)_9SO_2$]. [PPN]-[$HFe_3(CO)_{11}$] (**I**) cleanly reacts with 1 mol of SO_2 to produce the cluster [PPN][$HFe_3(CO)_9SO_2$] (**II**), eq 3, and CO. The back reaction, CO displacement of the SO_2 ligand in **II**, does not occur under a modest pressure of CO.

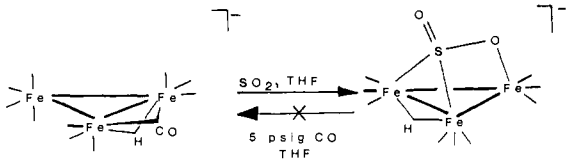

(3)

The formulation of **II** as [PPN][$HFe_3(CO)_9SO_2$] is substantiated by the FAB mass spectrum. The observed isotope distribution of the peaks with +2 m/z of the parent peak at 485

Table V. X-ray Crystal Structure Data for $[PPN]_2[Fe_3(CO)_9SO]$

formula	$Fe_3P_4SO_{11}N_2C_{84}H_{66}$
M	1602.95
cryst size, mm	0.4 × 0.3 × 0.3
cryst system	monoclinic
space group	*Cc* (#9)
a, Å	29.333(5)
b, Å	14.481(4)
c, Å	25.048(4)
β, deg	134.44(1)
V, Å^3	7597(6)
Z	4
d(calc), g cm^{-3}	1.401
μ(Mo K*α*), cm^{-1}	7.434
radiation	Mo K*α* (*λ* = 0.71069 Å)
scan type	*ω*–*θ*
2*θ* max, deg	45.0
unique data	6965
obsd data, (*I*) > 3*σ*(*I*)	5426
no. of variables	945
reflcn/parameter ratio	5.74
R(*F*)	0.034
$R_w(F)$	0.036
GOF	1.33

Table VI. Positional Parameters for Significant Atoms in $[PPN]_2[Fe_3(CO)_9SO]$

atom	*X*	*Y*	*Z*
Fe(1)	0.4074	0.67504(5)	0.1583
Fe(2)	0.28606(5)	0.68732(6)	0.03355(6)
Fe(3)	0.33344(5)	0.52948(5)	0.10311(6)
S(1)	0.32668(8)	0.6548(1)	0.1424(1)
O(1)	0.3106(3)	0.6786(5)	0.1826(3)
O(11)	0.4474(2)	0.6420(3)	0.0802(2)
O(12)	0.4424(3)	0.8683(3)	0.2015(3)
O(13)	0.5161(2)	0.6032(3)	0.3072(2)
O(21)	0.2925(2)	0.6431(3)	–0.0754(2)
O(22)	0.2910(3)	0.8874(3)	0.0276(3)
O(23)	0.1512(2)	0.6632(4)	–0.0524(3)
O(31)	0.2128(2)	0.4325(4)	0.0198(3)
O(32)	0.4223(2)	0.4177(3)	0.2382(2)
O(33)	0.3657(2)	0.4598(3)	0.0229(3)
C(11)	0.4314(3)	0.6536(4)	0.1105(3)
C(12)	0.4276(3)	0.7919(5)	0.1828(3)
C(13)	0.4729(3)	0.6296(4)	0.2480(3)
C(21)	0.2902(3)	0.6587(4)	–0.0325(3)
C(22)	0.2888(3)	0.8083(4)	0.0308(3)
C(23)	0.2036(3)	0.6711(5)	–0.0193(4)
C(31)	0.2599(3)	0.4724(4)	0.0528(3)
C(32)	0.3867(3)	0.4628(4)	0.1845(3)
C(33)	0.3531(3)	0.4893(4)	0.0541(4)

agrees closely with calculated distribution as shown by $R_p < 0.01$.[36] An infrared spectrum of **II** shows that bridging CO is no longer present. A mull infrared spectrum of **II** in Nujol reveals low frequency S–O stretches (1143, 929 cm^{-1}) in the range for an η^2 SO_2 ligand in mononuclear complexes.[37] Thus the IR data suggest that the SO_2 ligand is bound through both sulfur and oxygen to the metals.

The results of a single-crystal X-ray diffraction structure determination are summarized in an Ortep drawing of **II**, Figure 1, which reveals that the SO_2 bridges between two iron atoms through the sulfur and binds to the third through the oxygen. The three iron atoms form a $Fe_3(CO)_9$ triangle, and the coordination of the S is distorted to allow one oxygen to bend down toward Fe3.

The coordination of the SO_2 ligand in **II** is unusual but not unprecedented.[13,15] Typically SO_2 ligands in polynuclear complexes bridge two metals through the S atom, serving as formal 2-electron donors.[1] In **II**, the SO_2 must share 4 electrons with the metal atoms to satisfy the electron count of a trimetallic

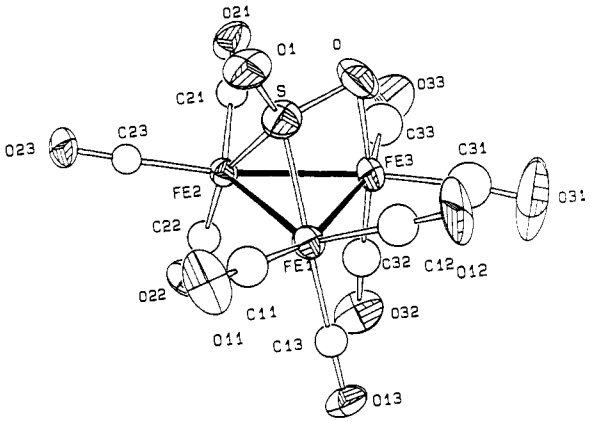

Figure 1. Ortep drawing of $[PPN][HFe_3(CO)_9SO_2]$. Ellipsoids are drawn at the 50% probability level.

cluster (48 e). A SO_2 ligand does not usually serve as a formal four-electron donor, as in **II**. Few clusters are known with SO_2 in this coordination mode. Two clusters with similarly bound SO_2 ligands are $[Rh_4(\mu\text{-}CO)_4(\mu\text{-}SO_2)_3(P(OPh)_3)_4]$[15] and $[Pd_5(\mu_2\text{-}SO_2)_2(PMe_3)_5]$.[13] The four shared electrons may come from the S and from a lone pair on the oxygen.

Bond distances and angles are shown in Tables III and IV. The distance between the S and the O bonded to Fe3 is much longer than the distance between the S and the *exo* oxygen and longer than distances observed in most η^2 mononuclear complexes, such as $RuCl(NO)(SO_2)(PPh_3)_2$ (S–O = 1.504(5), 1.459 Å).[38] Fe–Fe distances and Fe–S distances resemble those in the clusters $[PPN]_2[Fe_6C(CO)_{15}SO_2]$ and $[PPN]_2[Fe_3(CO)_7(SO_2)_2CCO]$.[17] The short S–O distance in **II** is similar to that found in free SO_2 (1.431(1) Å), but the long, 1.62 Å, S–O distance is much longer than that in the free ligand.[39] The long S–O distance is also longer than that in other SO_2 clusters with this coordination mode.[1,13,15]

Variable-temperature ^{13}C NMR spectra indicate that **II** has the same structure in solution and in the solid state. They also aid in the location of the hydrogen atom, which could not be directly located by X-ray crystallography. A single broad and temperature-independent resonance, found for the hydride at –15.74 ppm, indicates that the proton is bound to the metal framework. In solution II, has a plane of symmetry through S, O1, and Fe3, as shown by the ^{13}C NMR spectrum. No intrametallic exchange of the carbonyl ligands is observed by ^{13}C NMR at room temperature. A $^{13}C\{^1H\}$ spectrum of **II** taken at –90 °C (Figure 2) reveals resonances at 203.29, 215.18, and 215.55 ppm, which may be assigned to the carbonyls on Fe1 and Fe2. These resonances broaden at room temperature because of intrametallic exchange. Resonances at 211.14 and 216.45 ppm belong to the carbonyls on Fe3. These broaden and coalesce at higher temperatures, giving a single peak at 213.87 ppm at room temperature again because of intrametallic exchange. A ^{13}C proton-coupled spectrum acquired at –90 °C (Figure 2) reveals a splitting of the resonances at 203.80 ppm (*J*(C–H) = 2–3 Hz) and 215.6 ppm (*J*(C–H) = 11 Hz). This coupling, combined with the symmetry restrictions indicated by the ^{13}C NMR spectra, strongly suggests that the hydride bridges the Fe–Fe bond which also is bridged by the sulfur atom of the SO_2 ligand.

A space-filling model, generated on SYBYL from the crystallographic coordinates (Figure 3), supports this conclusion. An empty space for the hydride lies only between Fe1 and Fe2. Molecular modeling of metal carbonyl hydrides has previously

(36) Karet, G. B.; Espe, R. L.; Stern, C. L.; Shriver, D. F. *Inorg. Chem.* **1992**, *31*, 2658.
(37) Kubas, G. J. *Inorg. Chem.* **1979**, *18*, 182.
(38) Wilson, R. D.; Ibers, J. A. *Inorg. Chem.* **1978**, *17*, 2136.
(39) (a) Haase, J.; Winnewisser, M. *Z. Naturforsch.* **1968**, *23A*, 61. (b) Post, B.; Schwartz, R. S.; Fankuchen, I. *Acta Crystallogr.* **1952**, *5*, 372. (c) Morino, Y.; Kukuchi, Y.; Saito, S.; Hirota, E. *J. Mol. Spectros.* **1964**, *13*, 95.

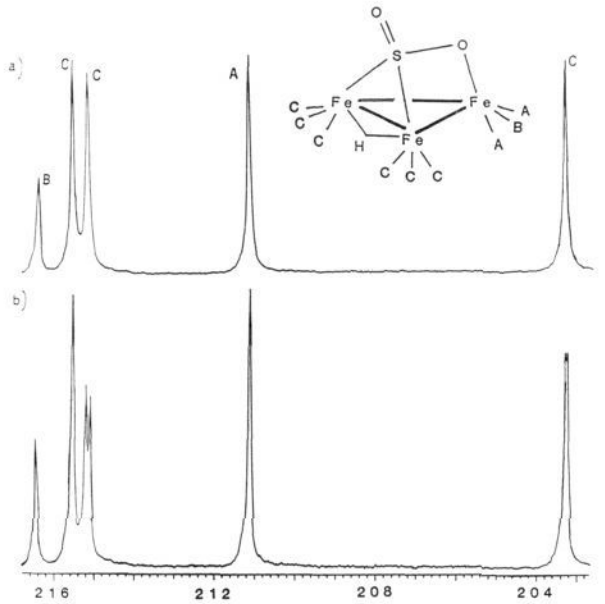

Figure 2. ^{13}C NMR spectra of $[PPN][HFe_3(CO)_9(SO_2)]$: (a) ^{13}C-{^1H} spectrum at –90 °C; (b) ^{13}C spectrum showing coupling of carbonyls to the hydride at –90 °C.

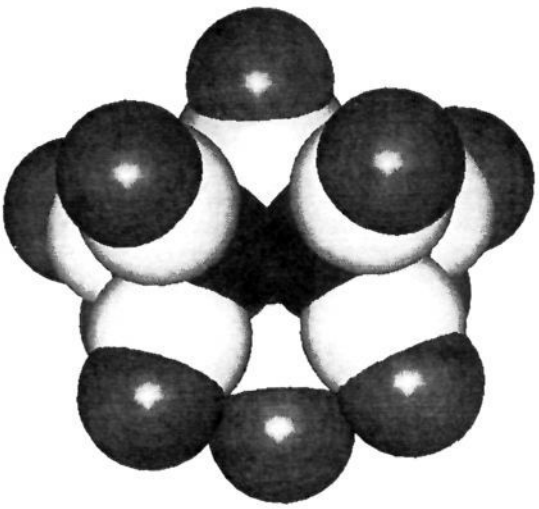

Figure 3. Space-filling diagram of $[PPN][HFe_3(CO)_9(SO_2)]$ showing a gap in carbonyl ligands where the hydride may fit. The SO_2 ligand is at the top of the picture.

been used to determine the probable positions of hydrogen atoms in this same manner.[40,41]

Electrochemistry of [PPN][HFe$_3$(CO)$_9$SO$_2$]. It is interesting to compare the electron withdrawing character of the η^2-SO_2 ligand with that of S-bonded SO_2 in other clusters. The most intense band for carbonyl stretching shifts from **I** to **II** about 15–20 cm^{-1}. This shift is significant but smaller than that of 20–30 cm^{-1} observed for the larger clusters $[PPN]_2[Fe_6C(CO)_{15}SO_2]$ and $[PPN]_2[Fe_5C(CO)_{13}SO_2]$ relative to $[PPN]_2[Fe_6C(CO)_6]$ and $[PPN]_2[Fe_5C(CO)_{14}]$.[17]

Cyclic voltammetric measurements were performed to compare the relative ease of oxidation and reduction of **I** and **II** with that of other SO_2 clusters. A strong irreversible oxidation peak was observed for **II** at Ep = 0.23 V versus Fc/Fc$^+$. Upon oxidation of **II**, an irreversible reduction wave occurred at Ep = 0.94 V versus Fc/Fc$^+$ which was not present without prior oxidation. Irreversible oxidation of $[PPN][HFe_3(CO)_{11}]$(**I**) occurred at Ep = –0.13 V versus Fc/Fc$^+$. After oxidation, a weaker, irreversible reduction peak appeared at Ep = 0.96 V versus Fc/Fc$^+$. As expected from the shifts in CO stretching frequencies, **II** is harder to oxidize than **I**. An explanation is that SO_2 withdraws more electrons from the cluster than CO.[17] For the clusters $[PPN]_2[Fe_6C(CO)_{15}]$ and $[PPN]_2[Fe_6C(CO)_{15}(SO_2)]$ and $[PPN]_2[Fe_5C(CO)_{13}(SO_2)]$ vs $[PPN]_2[Fe_5C(CO)_{13}(SO_2)]$, the SO_2 substituted clusters were also found to be harder to oxidize and easier to reduce than the unsubstituted clusters.[17]

Acetylation and Reduction of [PPN][HFe$_3$(CO)$_9$SO$_2$]. Reaction of **II** with *AcCl* followed by reduction with *NaPh$_2$CO* results in the formation of $[Fe_3(CO)_9S]^{2-}$ (**III**), which cocrystallizes with $[PPN]^+$ and Na^+ salts of the anion $[OAc]^-$. Cluster **III** was identified by IR, ^1H, and ^{13}C NMR spectra, which match those reported in the literature for $[PPN]_2[Fe_3(CO)_9S]$.[44] Furthermore, no terminal S–O stretch was observed for **III**. No hydride resonance was found in the ^1H NMR spectrum, although free OAc^- was identified in solution.

The acetylated intermediate, which could not be isolated as a solid due to its instability, was characterized in situ by ^1H and ^{13}C NMR spectroscopy and by IR spectroscopy. Carbonyl stretching frequencies indicate a neutral species (ν(CO) 2080 (w), 2062 (m), 2047 (s), 2006 (s), 1979 (m), 1962 (w), 1908 (w) cm^{-1}). Also present is a band at 1748 cm^{-1} for the C–O stretch in the acetyl group. ^1H and ^{13}C NMR spectra (CD_2Cl_2, 20 °C) show the formation of two products, **VII** and **VIII**. The NMR spectra for **VII**, normally a minor product, contain ^1H resonances at 2.23 and -24.44 ppm and ^{13}C resonances (25 °C) at 202.54, 167.29, and 20.49 ppm. Resonances at 2.23 (^1H), 20.49 (^{13}C), and 167.29 (^{13}C) ppm correspond to the methyl hydrogens, the methyl carbon, and the carbonyl carbon, respectively, of the $CH_3C(O)$. The ^1H resonance at –24.44 ppm may be assigned to the hydride ligand. A peak at 202.54 ppm corresponds to the carbonyl carbons. The second product, **VIII**, normally the majority product, contains resonances for the oxygen-bound acetate group at 2.25 ppm (^1H $CH_3C(O)$) and ^{13}C resonances at 166.78 ($CH_3C(O)$) and 20.2 ppm ($CH_3C(O)$). These resonances are in the range reported for oxygen bound $CH_3C(O)$ in $[PPN][Fe_3(CO)_9CCOAc]$ (^1H, 2.30 ppm; ^{13}C, 168.1 and 20.6 ppm).[43] A hydride resonance is observed at –22.75 ppm. At room temperature, one resonance at 210.4 ppm is observed for the carbonyls. This resonance splits into two broad peaks at 215 (2 CO's) and 209 ppm (7 CO's) at –90 °C. The formation of OAc^- along with $[Fe_3(CO)_9S]^{2-}$ supports the conclusion that the $CH_3C(O)Cl$ attacks an O atom.

Because the carbonyl stretching frequencies are much higher than normally observed for CO ligands that can undergo electrophilic attack, the probable site for reaction of the $CH_3C(O)^+$ with the cluster is the SO_2 ligand. For example, in the acetylation and reduction of bridging carbonyl ligands in $[PPN]_2[Fe_4(CO)_{13}]$ and $[PPN]_2[M_3(CO)_{11}]$ (M = Fe, Ru, Os), ν(CO)

(40) (a) McPartlin, M.; Eady, C. F.; Johnson, B. F. G.; Lewis, J. *J. Chem. Soc., Chem. Commun.* **1976**, 883. (b) Johnson, B. F. G.; Lewis, J.; Nelson, W. J. H.; Vargas, M. D.; Braga, D.; Henrick, K.; McPartlin, M. *J. Chem. Soc., Dalton Trans.* **1984**, 2151.

(41) Orpen, A. G. *J. Chem. Soc., Dalton Trans.* **1980**, 2509.

(42) (a) Markó, L.; Takács, J.; Papp, S.; Markó-Monostory, B. *Inorg. Chim. Acta* **1980**, *45*, L189. (b) Markó, L.; Madach, T.; Vahrenkamp, H. *J. Organomet. Chem.* **1980**, *190*, C67.

(43) (a) Bockman, T. M.; Wang, Y.; Kochi, J. K. *New J. Chem.* **1988**, *12*, 387. (b) Fischer, K.; Deck, W.; Schwartz, U.; Vahrenkamp, H. *Chem. Ber.* **1985**, *118*, 4946. (c) Imhof, W.; Hüttner, G.; Eber, B.; Guenauer, D. *J. Organomet. Chem.* **1992**, *428*, 379. (d) Winter, A.; Zsolnai, L.; Hüttner, G. *J. Organomet. Chem.* **1982**, *234*, 337. (e) Faessler, T.; Hüttner, G. *J. Organomet. Chem.* **1989**, *376*, 367. (f) Bockman, T. M.; Kochi, J. K. *J. Am. Chem. Soc.* **1987**, *109*, 7725.

(44) Hriljac, J.A. Ph.D. Thesis, Northwestern University, 1987.

for the carbonyls which undergo electrophilic attack is much less than 1900 cm^{-1}.[22] However, in $[PPN][HFe_3(CO)_9(SO_2)]$, no bridging CO's are present and there is no C–O stretch at a frequency lower than 1959 cm^{-1}. Furthermore, the lack of low C–O IR stretches or downfield carbonyl ^{13}C NMR resonances in **VIII** indicates that terminal carbonyl ligands in **II** have not been induced into bridging positions upon electrophilic attack.

In mononuclear or dinuclear complexes formed by the interaction of an electrophile with an η^2-SO_2 ligand, the SO_2 is generally bonded to the electrophilic fragment through the *exo* oxygen. For example, in $[Ru(CO)_2(\eta^2\text{-}SO_2\cdot SO_2)(PPh_3)_2]$, a second SO_2 molecule acts as a Lewis acid, binding through S to the oxygen of the coordinated SO_2 that is not bonded to the ruthenium.[20] Likewise, the formation of $[Mo(CO)_2(PPh_3)(py)(\mu\text{-}SO_2)]_2$ by dimerization of $[Mo(CO)_2(PPh_3)(py)(\eta^2\text{-}SO_2)]$ may be viewed as the electrophilic attack of a Mo fragment on the *exo* oxygen of an η^2-SO_2 ligand.[1,11] For this reason AcCl is proposed to attack at the *exo* oxygen of the η^2-SO_2 in $[PPN][HFe_3(CO)_9SO_2]$, **VIII**.

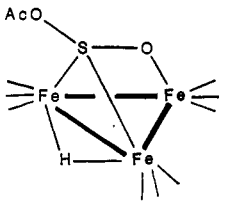

VIII

The reaction of **VIII** with progressive addition of $NaPh_2CO$, as followed by IR spectroscopy, revealed three sequential intermediates. A logical course for this reaction is stepwise S–O bond cleavage accompanied by reduction of the H ligand. The compounds $[H_2Fe_3(CO)_9S]$ and $[PPN][HFe_3(CO)_9S]$[42,44] are known, but they are not observed in the reaction mixture as intermediates. Removal of the hydride ligand from the protonated sulfido cluster is therefore most likely not the final step. A logical first step might be cleavage of the acetylated SO_2 oxygen atom to generate a monoanionic cluster (ν(CO), THF, main band at 2012 cm^{-1}), $[PPN][HFe_3(CO)_9SO]$. Reaction with sodium benzophenone might then proceed with concurrent removal of the hydride and cleavage of the second oxygen.

This type of reaction may be compared to the reductive cleavage reactions of CO. In the proton-induced reduction of CO in $[PPN]_2[Fe_4(CO)_{13}]$, the C–O bond is weakened and then reductively cleaved to produce a carbide cluster.[45] Additionally, the C–O bond of bridging carbonyl ligands in the clusters $[PPN]_2[M_3(CO)_{11}]$ (M = Fe, Ru, Os) and $[PPN]_2[Fe_4(CO)_{13}]$ may be cleaved by attack of $CH_3C(O)$ followed by reduction with $NaPh_2CO$.[22]

Synthesis and Characterization of $[PPN]_2[Fe_3(CO)_9(SO)]$ (IX). Reduction of **II** without prior acetylation leads to the formation of $[PPN]_2[Fe_3(CO)_9SO]$ in moderate yields (eq 5). The cluster **IX** is not observed as an intermediate in the reduction of $[Fe_3(CO)_9(SO_2Ac)]$ by infrared spectroscopy. Addition of excess reducing agent to $[PPN]_2[Fe_3(CO)_9SO]$ results in degradation of the cluster rather than formation of $[PPN]_2[Fe_3(CO)_9S]$.

An Ortep drawing of **IX**, Figure 4, shows that the SO ligand bridges symmetrically across all three iron atoms. Bond distances and angles (Tables VII and VIII) reveal that the three iron atoms form an equilateral triangle with the SO centered above it. Only small variations in Fe–Fe and Fe–S distances are seen. Fe–Fe and Fe–S distances are comparable to those in $[PPN][HFe_3(CO)_9(SO_2)]$, $[PPN]_2[Fe_6C(CO)_{15}(SO_2)]$, and $[PPN]_2[Fe_3(CO)_7(SO_2)_2CCO]$.[17]

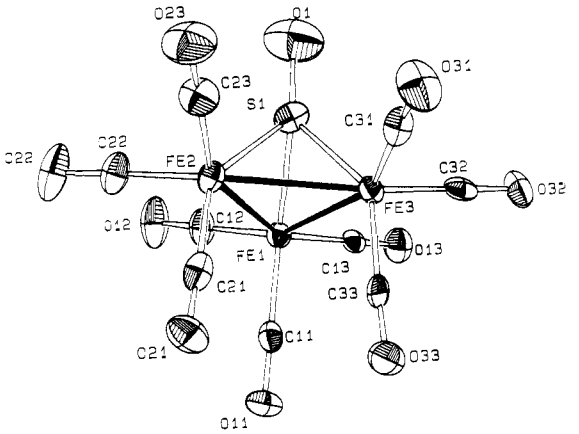

Figure 4. Ortep drawing of $[PPN]_2[HFe_3(CO)_9SO]$ (**IX**). Ellipsoids are drawn at the 50% probability level.

Table VII. Selected Bond Distances (Å) in $[PPN]_2[Fe_3(CO)_9SO]$ (IX)

Fe1–Fe2	2.625(1)	Fe2–C21	1.791(7)	O12–C12	1.159(7)
Fe1–Fe3	2.619(1)	Fe2–C22	1.757(6)	O13–C13	1.150(6)
Fe1–S1	2.128(2)	Fe2–C23	1.781(7)	O21–C21	1.146(7)
Fe1–C11	1.791(6)	Fe3–S1	2.139(2)	O22–C22	1.153(7)
Fe1–C12	1.756(7)	Fe3–C31	1.766(7)	O23–C23	1.131(8)
Fe1–C13	1.768(6)	Fe3–C32	1.752(6)	O31–C31	1.152(7)
Fe2–Fe3	2.608(1)	Fe3–C33	1.780(6)	O32–C32	1.166(7)
Fe2–S1	2.128(2)	S1–O1	1.422(6)	O33–C33	1.155(7)
		O11–C11	1.150(7)		

Table VIII. Selected Bond Angles (deg) for $[PPN]_2[Fe_3(CO)_9SO]$

Fe2–Fe1–Fe3	59.64(3)	Fe2–Fe3–S1	52.12(5)
Fe2–Fe1–S1	51.90(5)	Fe1–S1–Fe2	76.16(6)
Fe3–Fe1–S1	52.31(5)	Fe1–S1–Fe3	75.74(6)
Fe1–Fe2–Fe3	60.07(3)	Fe1–S1–O1	135.3(3)
Fe1–Fe2–S1	51.93(5)	Fe2–S1–Fe3	75.37(6)
Fe3–Fe2–S1	52.51(5)	Fe2–S1–O1	133.5(3)
Fe1–Fe3–Fe2	60.29(4)	Fe3–S1–O1	135.7(3)
Fe1–Fe3–S1	51.95(5)		

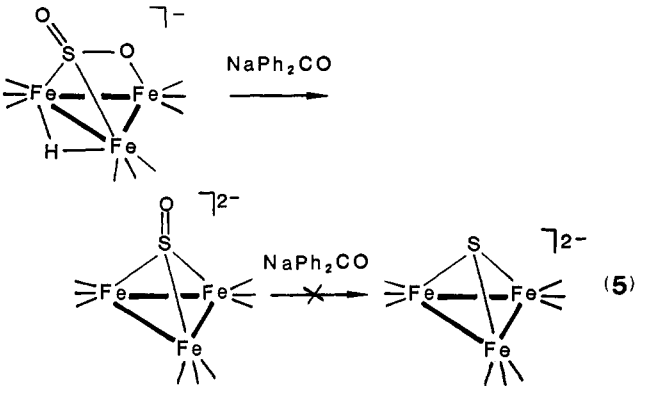

(5)

The S–O distance (1.422 Å) is similar to that in free SO_2, indicating a strong S–O bond.[39] It is slightly shorter than the S–O distance in free SO.[25a] This distance also compares favorably to that of 1.471(2) Å in $[Fe_3(CO)_7SSO]$.[27] In order to satisfy the electron count of **IX**, the SO ligand must serve as a 4-electron donor; SO often donates 4 electrons when it bridges metal–metal bonds.[3]

A ^1H NMR spectrum gives no evidence for the continued presence of the hydride ligand. 13C NMR data indicate that $[PPN]_2[Fe_3(CO)_9(SO)]$ has a C3 axis through the SO ligand in solution. Two temperature-independent resonances are observed for **IX** at 221.8 (6 CO's) and 219.7 (3 CO's) ppm. The resonance

(45) (a) Whitmire, K.; Shriver, D. F. *J. Am. Chem. Soc.* **1980**, *102*, 1456. (b) Manassero, M.; Sansoni, M.; Longoni, G. *J. Chem. Soc., Chem. Commun.* **1976**, 919. (c) Horowitz, C. P.; Shriver, D. F. *Adv. Organomet. Chem.* **1984**, *23*, 219.

at 221.8 ppm may be assigned to two carbonyls on each iron atom and that at 219.7 ppm to one carbonyl on each iron. The lack of carbonyl exchange at room temperature is an unusual feature of this cluster.

Only two complexes with three or more metals and SO ligands have been crystallographically characterized, $[Co_4S_3(SO)(CN)_{12}]^{8-}$ and $[Fe_3(CO)_9(SO)S]$.[27,46] On the basis of bond distances and ν(SO), the SO ligand in the Co cluster was formulated as SO^{2-}. A third cluster, $[Fe_3Pt(CO)_6(PPh_3)_2S(SO)]$, was identified by sulfur–oxygen stretches, mass spectrometry, and ^{31}P NMR data.[47] All of these clusters were postulated to arise from oxidation of a sulfide ligand. The cluster **IX**, however, was made by reductive cleavage of SO_2 and is the only electron rich, reduced sulfur monoxide cluster known. The only example of reduction of SO_2 to SO of which we are aware occurs in the A-frame complex $[Ir_2(CO)_2(dppm)H_4]$.[48] This complex reacts with SO_2 to produce an unstable SO complex, which decomposes to a dimer containing a sulfide ligand and a small amount of another SO complex.

A mull infrared spectrum of $[PPN]_2[Fe_3(CO)_9(SO)]$ (**IX**) reveals an S–O stretch at 1038 cm^{-1}. This stretch is lower than that observed at 1123 cm^{-1} for free SO.[25] In other SO complexes ν(SO) ranges from 883 to 1150 cm^{-1}. Most S–O stretches are found between 1000 and 1150 cm^{-1}, with only a few outside of this region. $[Fe_3(CO)_9S(SO)]$ and $[Fe_2Pt(CO)_6(PPh_3)_2(SO)]$ have stretches at 1103 and 1058 cm^{-1}, respectively.[27,47] Thus the ν(SO) in **IX** is somewhat lower than that found in other carbonyl clusters. The cluster $K_8[Co_4S_3(SO)(CN)_{12}]$, containing SO^{2-}, has a low stretch at 995 cm^{-1}.[46]

Because of the paucity of data on S–O bond lengths in sulfur monoxide complexes, the correlation of ν(SO) with S–O distances is not possible. Interestingly, ν(SO) in mononuclear and dinuclear sulfur monoxide complexes varies with the electron count of the metal complex and the location of the metal in the periodic table (Table IX). Thus the 18-electron Fe and Ru complexes have a lower ν(SO) than the 18-electron Ir complexes. The S–O stretches of 16-electron Ir and Rh sulfur monoxide complexes lie between 1058 and 1072 cm^{-1}, but those of the 18-electron Ir complexes occur at 1114–1126 cm^{-1}. In 36-electron dimetallic complexes the Mn dimers have a lower ν(SO) than the Ir dimers. Three dimetallic complexes, which, according to the structures indicated by the authors, have 34 electrons, all have very low S–O stretches in comparison to the other dimetallic complexes.

Table IX. ν_{SO} of Sulfur Monoxide Complexes

complex	ν_{SO}, cm^{-1}	bonding mode of SO_2	ref
16-Electron Complexes			
$[Rh(PCy_3)_2Cl(SO)]$	1072	bent	49
$[Ir(PCy_3)_2Cl(SO)]$	1070	bent	49
$[Ir(PiPr_3)_2Cl(SO)]$	1071	bent	26
$[Rh(PiPr_3)_2Cl(SO)]$	1075	bent	26
$[Rh(C_5H_5)(SO)]$	1044	linear or bent	50
$[Rh(C_5H_4Me)(SO)]$	1024	linear or bent	50
$[Pd(Ph_3P)_2(SO)]$	1058	bent	51
18-Electron Complexes			
$[Cp'Ru(PMePh_2)(CO)(SPh)]$	1056	bent	52
$[Cp'Fe(PMe_3)_2(SO)]^+$	1046	bent	53
$[CpFe(cdpe)(SO)]^+$	1055	bent	53
$[Cp'Ru(Me_3P)_2(SO)]^+$	1064	bent	53
$[Cp'RuCl(PiPr_3)(SO)]$	1066	bent	54
$[Cp'RuCl(PCy_3)(SO)]$	1065	bent	54
$[CpFe(dppe)(SO)]^+$	1062	bent	55
$[((PhO)_3P)_2(CO)_2Fe(SO)]$	1088	bent	31
$Ir(PiPr_3)_2Cl(SO)(H)_2]$	1122	bent	56
$[Ir(PPhiPr_2)_2Cl(SO)(H)_2]$	1126	bent	56
$[IrCl_2H(PiPr_3)_2(SO)]$	1114	bent	56
34-Electron Dimeric Complexes			
$[Pd_2Cl_2(SO)(dpm)_2]$	985	μ_2, η^1	57
$[Pd_2Cl_2(SO)(dpm)(dpMe)]$	984	μ_2, η^1	57
$[Rh_2(CO)_2(dppm)_2(SO)]$	883	μ_2, η^1	58
36-Electron Dimeric Complexes			
$[CpMn(CO)_2]_2(SO)$	1037–1045	μ_2, η^1	28
$[Cp'Mn(CO)_2](SO)$	1031	μ_2, η^1	59
$[Mn(CO)_4(PPh_3)]_2(SO)$	1032	μ_2, η^1	30
$[Ir_2(CO)_2H_2(dmpm)_2(SO)]$	1135	μ_2, η^1	48
$[Ir_2(CO)_2(dmpm)_2(SO)]$	1150	μ_2, η^1	48
Cluster Complexes			
$[PPN]_2[Fe_3(CO)_9SO]$	1038	μ_3, η^1	
$[Fe_3(CO)_9S(SO)]$	1103–1107	μ_3, η^1	27, 32
$[Fe_2Pt(CO)_6(PPh_3)_2(SO)]$	1058	μ_3, η^1	47
$K_4[Co_4S_3(SO)(CN)_{12}]$	995	μ_3, η^1	46

Conclusions

Cluster bound sulfur dioxide may be reduced to sulfido or sulfur monoxide ligands in the cluster $[PPN][HFe_3(CO)_9SO_2]$. Acetylation of the cluster **II** is necessary for reductive cleavage of both oxygens from sulfur dioxide. Sulfur dioxide differs from CO in that some reductive S–O cleavage may occur without prior electrophilic attack to weaken the S–O bond and to convert the oxygen into a good leaving group. Reduction of $[HFe_3(CO)_9(SO_2Ac)]$ occurs via a complex, multistep mechanism which does not appear to involve formation of $[PPN][HFe_3(CO)_9S]$ or $[PPN]_2[Fe_3(CO)_9SO]$ intermediates.

Acknowledgment. We acknowledge support of this work by the U.S. Department of Energy Award No. DE-FG02–86ER13640. Support for D. M. N. was provided by the National Science Foundation Award No. CHE-9014662. G. B. K. thanks R. L. Espe for helpful discussions.

Supplementary Material Available: Listing of a set of positional parameters of all atoms and a complete list of bond distances and angles and thermal parameters for **II** and **IX** (22 pages); structure factor tables for **II** and **IX** (53 pages). Ordering information is given on any current masthead page.

(46) Müller, A.; Krickmeyer, E.; Jostes, R.; Bögge, H.; Dieman, E.; Bergman, U. *Z. Naturforsch.* **1985**, *40B*, 1715.
(47) Hoots, J. E.; Lesch, D. A.; Rauchfuss, T. B. *Inorg. Chem.* **1984**, *23*, 3130.
(48) Neher, A.; Lorenz, I. P. *Angew. Chem., Int. Ed. Engl.* **1989**, *28*, 1342.
(49) Schenk, W. A.; Leissner, J.; Burschka, C. *Z. Naturforsch.* **1985**, *40B*, 1264.
(50) Heyke, O.; Lorenz, I.-P. *Phosphorus, Sulfur, and Silicon* **1992**, *71*, 139.
(51) Heyke, O.; Neher, A.; Lorenz, I.-P. *Z. Anorg. Allg. Chem.* **1992**, *608*, 23.
(52) Schenk, W. A.; Dombrowski, E.; Reuther, I.; Stur, T. *Z. Naturforsch.* **1992**, *47B*, 732.
(53) Schenk, W. A.; Karl, U.; Horn, M. R.; Müssig, S. *Z. Naturforsch.* **1990**, *45B*, 239.
(54) Schenk, W. A.; Karl, U. *Z. Naturforsch.* **1989**, *44B*, 988.
(55) Schenk, W. A.; Müssig, S. *J. Organomet. Chem.* **1987**, *320*, C23.
(56) Schenk, W. A.; Leissner, J. *Z. Naturforsch.* **1987**, *42B*, 967.
(57) Besenyei, G.; Lee, C.-L.; Gulinski, J.; Rettig, S. J.; James, B. R.; Nelson, D. A.; Lilga, M. A. *Inorg. Chem.* **1987**, *26*, 3622.
(58) Neher, A.; Heyke, O.; Lorenz, I.-P. *Z. Anorg. Allg. Chem.* **1989**, *578*, 185.
(59) Heberhold, M.; Schmidkonz, B. *J. Organomet. Chem.* **1986**, *308*, 35.